Progress In Electromagnetics Research M, Vol. 99, 139–152, 2021

Contrast in Specific Absorption Rate for a Typical Plant Model due to Discrepancy among Global and National Electromagnetic Standards

Ardhendu Kundu[1, *], Bhaskar Gupta[1], and Amirul I. Mallick[2]

Abstract—Different global and national electromagnetic regulatory standards have been developed based upon significantly diversified premises, developmental backgrounds, and objectives to safeguard life. Some standards aim at minimizing short duration thermal effects; some try to mitigate non-thermal effects over prolonged duration; and rest have adopted precautionary limits. As a consequence, these global and national electromagnetic standards substantially differ from each other. Moreover, in spite of lossy dielectric nature of plant tissues, electromagnetic energy absorption rate level estimations for a complete plant model have neither been reported in literature nor been considered while preparing safety standards. To this end, Specific Absorption Rate levels have been estimated for a typical *Catharanthus roseus* plant model — typical geometric shape of the plant prototype has been modelled considering the most practical scenario. Detailed analyses on variation of Specific Absorption Rate levels due to wide discrepancy among the existing electromagnetic regulatory standards have been reported in a quantitative manner. This particular work encompasses dielectric properties measurement of different *Catharanthus roseus* plant samples, modelling a typical *Catharanthus roseus* plant containing leaves, flower, and twig with appropriate dielectric properties defined, and finally the simulation-based investigations to estimate the variation in Specific Absorption Rate levels based on the contrasting electromagnetic exposure standards. Specific Absorption Rate levels have been reported at five different telecommunication bands as per two occupational and four public exposure scenarios. Variations among the estimated Specific Absorption Rate levels have been noted to be significant and presented in detail in this article. A total of thirty rigorous simulations have been carried out along with one hundred and twenty Specific Absorption Rate data evaluations to ensure accurate comparison among different electromagnetic standards. Noted vast variations among estimated Specific Absorption Rate levels based on contrasting electromagnetic standards over the frequencies indicate the necessity of re-evaluating all existing guidelines and also call for the need of maintaining a global uniformity among the existing electromagnetic standards worldwide.

1. INTRODUCTION

Several global and national electromagnetic regulatory standards are currently effective in different parts of the world [1–10]. There are substantial differences in the premises, backgrounds (such as technical specifications and medical practices), and purposes of these regulatory standards. Some electromagnetic standards have been developed based on assessing thermal effects of electromagnetic radiation over short time span, and some other standards aim at mitigating non-thermal effects over prolonged exposure duration whereas rest are prescribed to take adequate precautions against yet

Received 4 September 2020, Accepted 24 November 2020, Scheduled 7 December 2020
* Corresponding author: Ardhendu Kundu (ardhendukundu.1989@gmail.com).
[1] Department of Electronics and Telecommunication Engineering, Jadavpur University, Kolkata, India. [2] Department of Biological Sciences, Indian Institute of Science Education and Research Kolkata, India.

unknown health effects [11]. However, each standard is consistent with the policy promoted by the respective regulatory organization. To name a few organizations that prescribed global electromagnetic exposure standards, Federal Communications Commission (FCC) [1], International Commission on Non-Ionizing Radiation Protection (ICNIRP) [2] and Institute of Electrical and Electronics Engineers (IEEE) [3] secure the top ranks. In contrast, India [4], Switzerland [5], Russia [6], Italy [7, 8], etc. are among the selected countries to enforce stricter national electromagnetic regulatory standards [9–11]. National electromagnetic exposure guidelines are made stricter to address possible health concerns raised by researchers and awareness among common people in selected countries — stricter national protocols are adopted either based on scientific basis or to take precautions [11]. However, there is lack of uniformity among the different global and national electromagnetic exposure standards resulting in ten to hundred fold variations in plane wave equivalent reference power density levels across countries over several telecommunication bands. Let one consider 1842.5 MHz (center frequency of 1805–1880 MHz downlink band) for an example. The plane wave equivalent reference power density levels adopted by FCC [1], ICNIRP [2], India [4], and Switzerland [5] are $10\,\mathrm{W/m^2}$, $9.21\,\mathrm{W/m^2}$, $0.92\,\mathrm{W/m^2}$, and $0.092\,\mathrm{W/m^2}$, respectively [9–11]. As a consequence, living objects, i.e., humans, animals, as well as plants, are expected to absorb significantly different amounts of Radio Frequency (RF) energy due to mobile tower emitted uninterrupted pulsed microwave radiation depending upon the electromagnetic regulatory standards in effect. Stringent public exposure scenarios in countries like Russia, Italy, etc. (fixed at $0.10\,\mathrm{W/m^2}$ from $\leq 300\,\mathrm{MHz}$ to $300\,\mathrm{GHz}$) are also at comparable scale to that of Swiss public standard [5–8]. It should be noted that Specific Absorption Rate (SAR) is used as a metric of the rate at which RF energy is absorbed by a living object while being exposed to an incident electromagnetic wave. It is defined as the amount of power absorbed per unit mass of tissue and has units of watts per kilogram (W/kg) or milliwatts per gram (mW/g). It is in general averaged either over a small sample tissue (like point mass, 1 g or 10 g) or over the whole body [1, 2]. Mathematically, SAR at a point is defined as $\sigma|E|^2/2\rho$, where σ is the electrical conductivity of biological tissue, $|E|$ the maximum value of time varying continuous wave electric field at the point of interest inside tissue, and ρ the tissue density. For uninterrupted pulsed microwave incidence on biological object, equivalent continuous wave electric field strength can be derived from the duty cycle of the pulse train. Thereafter, $|E|$ at the point of interest inside biological tissue can be evaluated further to calculate point SAR value.

Assessing RF energy absorption in human phantoms and subsequent SAR estimation remain an established research domain worldwide [12–25]. Dependence of SAR on frequency and polarization of electromagnetic field [12], frequency, power density and time of exposure [13], equivalent dielectric properties of human phantom model [14], distance, frequency and human tissue composition [15], minimum distance from cell tower antennas [16], placement, i.e., height and tilt angle of phone near human torso [17], size of human head during childhood [18], different human organs (like eye, testis, brain, and kidney) [19], electrical properties of human tissue along with surface area [20], different homogeneous models of nine month old infant [21], flat human phantom modelling [22], different multilayer anatomical models, and external field strength [23], etc. have been reported in literature. Moreover, temperature distributions in human head [24] and eye [25] models have also been reported due to electromagnetic energy absorption. Likewise, plants, vegetables, and fruits also possess dielectric properties that indicate a consistent absorption of the RF energy in wireless communication bands. Free space transmission technique and open ended coaxial probe technique have been primarily reported for dielectric properties characterization of different crop, vegetable, fruit and plant samples [26–32]. In addition, SAR data have been reported as per ICNIRP [33, 34], FCC [35], and revised Indian [36–40] electromagnetic regulatory guidelines for different fruit models in recent times. However till date, SAR data and its surface distribution for a complete plant model are not available in literature.

Combining these aspects together, this work aims at highlighting the wide discrepancies among different global and national electromagnetic regulatory standards, characterizing dielectric properties of plant samples, investigating SAR distribution in a typical plant model (containing leaves, flower and stem) for plane wave incidence along with analyzing the contrast in SAR data due to discrepancy among different global and national electromagnetic standards over a number of frequency bands [1, 2, 4, 5]. To this notion, *Catharanthus roseus* plant containing green leaves, green stem, and pink flower have been chosen as prototype. Dielectric properties of fresh leaf, flower, and stem samples have been characterized using open ended coaxial probe technique [28–32]. Next, a typical three-dimensional

Catharanthus roseus plant model has been developed. SAR data have been simulated as per established electromagnetic regulatory standards prescribed by ICNIRP (international), FCC (international), India (national), and Switzerland (national) [1, 2, 4, 5]. At last, simulated SAR data have been compared at mid frequencies of multiple communication bands like 947.5 MHz (935–960 MHz downlink band), 1842.5 MHz (1805–1880 MHz downlink band), 2150 MHz (2120–2170 MHz downlink band), 2350 MHz (2300–2400 MHz band), and 2450 MHz (2400–2500 MHz band). Furthermore, how fixing a global set of criteria for investigating biological effects of electromagnetic radiation can lead to the path of minimizing the existing discrepancies among different electromagnetic standards has been discussed.

Section 2 of this article deals with material density and dielectric properties characterization techniques for biological tissues. This is followed by the computer aided design of a typical *Catharanthus roseus* plant model and computational electromagnetic scheme for SAR simulation in Section 3. The discrepancies among different electromagnetic regulatory standards have been detailed in Section 4. Collective results along with detailed discussions are presented in Section 5 followed by the conclusions, acknowledgment, and the list of references.

2. MATERIAL DENSITY AND DIELECTRIC PROPERTIES MEASUREMENT OF *CATHARANTHUS ROSEUS* PLANT

2.1. Material Density Measurement of *Catharanthus roseus* Plant Samples

Initially, a few typical medium sized fresh *Catharanthus roseus* plants have been collected. Thereafter, mass and volume of leaf, flower, and stem samples have been measured repetitively; material densities have been calculated by taking the ratio of mass to volume of respective samples. Finally, mean material density for each type of *Catharanthus roseus* sample is tabulated in Table 1.

Table 1. Measured material density (ρ) of *Catharanthus roseus* leaf, flower and stem samples.

Name of sample	Leaf	Flower	Stem
Material density (Kg/m^3)	717	267.7	774

2.2. Dielectric Properties Measurement of *Catharanthus roseus* Plant Samples

A number of dielectric measurement techniques are available for different types of materials; however, open ended coaxial probe technique has been widely accepted for characterizing dielectric properties of biological samples that are primarily soft solid, semi-solid or liquid in nature [28–32]. Open ended coaxial probe can be modelled as parallel combination of one fringing capacitance from inner to outer conductor through biological sample, one radiation conductance signifying propagation loss through biological sample along with another fringing capacitance from inner to outer conductor via intervening material within the coaxial structure. Values of fringing capacitance and conductance depend upon dielectric properties of material under test along with frequency of operation for a particular probe with known dimensions. Complex input admittance of the above mentioned probe is dependent upon radiation conductance (associated with real part) and fringing capacitance (associated with imaginary part) through the material under test. All physical and mathematical analyses of this particular technique are well established in literature [41–48] and have been further summarized in a recent article [40].

The following steps are exercised to measure dielectric properties of unknown material using open ended coaxial probe technique.

(1) During calibration, complex input admittance is measured in terms of reflection coefficient with Vector Network Analyzer (VNA) for reference samples (air and distilled water) with known dielectric properties.

(2) Measured complex input admittance and known complex permittivity data of the reference samples are utilized to calculate radiation conductance and fringing capacitance values in air.

(3) Later on, those parameters are further utilized to evaluate dielectric properties of unknown sample.

Real part of permittivity (ε') and loss tangent ($\tan\delta$) data for *Catharanthus roseus* leaf, flower, and stem samples have been measured with Agilent Technologies 85070E open ended coaxial probe (high temperature probe, $-40°$C to 200°C, option 020) and Agilent Technologies E5071B VNA. The dielectric measurement kit consists of a high temperature coaxial probe that can characterize dielectric properties up to 20 GHz. This particular probe is capable of characterizing dielectric properties for solid (with a smooth flat surface), semi-solid, and liquid samples possessing relatively high loss tangent (greater than 0.05). Dielectric parameters are computed from raw reflection coefficient data for material under test after calibrating the measurement set up at 25°C [31]. *Catharanthus roseus* leaves, flowers, and green stems consist of soft tissues with significant amount of liquid content. With individual leaf or flower sample being quite thin, sufficient number of leaves or flowers have been stacked, and thereafter, the coaxial probe is moderately pressed on stacked samples to avoid air gap between leaves or flowers to obtain accurate dielectric properties. Leaf or flower samples are stacked to provide sufficient material depth (depending upon skin depth) beneath the coaxial probe for accurate measurement. In the case of stem samples, a small amount of air gap could not be avoided due to cylindrical shape. Precaution has been taken during measurement because excessive pressure on the plant samples can cause tissue deformation resulting in erroneous measurement data.

Dielectric properties for above mentioned plant samples have been measured from 20 MHz to 8.5 GHz. To keep the data consistent with this work of SAR computation, permittivity (ε') and loss tangent ($\tan\delta$) parameters are tabulated in Table 2 at frequencies of interest. Dielectric properties measurement set up with plant samples is illustrated in Fig. 1(a) and Fig. 1(b), respectively.

Table 2. Measured dielectric properties of *Catharanthus roseus* leaf, flower and stem samples.

Sample	947.5 MHz		1842.5 MHz		2150 MHz		2350 MHz		2450 MHz	
	ε_r	$\tan\delta$	ε_r	$\tan\delta$	ε_r	$\tan\delta$	ε_r	$\tan\delta$	ε_r	$\tan\delta$
Leaf	57.85	0.501	54.05	0.331	53.53	0.306	53.21	0.295	53.21	0.295
Flower	62.47	0.212	60.53	0.175	60.14	0.182	60.03	0.186	60.04	0.186
Stem	43.26	0.475	40.16	0.326	39.47	0.315	39.29	0.307	39.29	0.307

(a) (b)

Figure 1. Dielectric properties measurement set up for *Catharanthus roseus* leaf samples with Agilent 85070E dielectric measurement kit and Vector Network Analyzer (VNA).

3. MODELLING A TYPICAL *CATHARANTHUS ROSEUS* PLANT AND COMPUTATIONAL SCHEME FOR SAR EVALUATION

3.1. CAD Modelling of a Typical *Catharanthus roseus* Plant

A few typical medium sized *Catharanthus roseus* plants have been collected; thereafter length, width, surface area, and radii of plant leaf, flower, and stem samples have been measured. Next, two dimensional

Table 3. Modelling specifications of *Catharanthus roseus* leaf, flower and stem samples.

Leaf Samples Specifications			
Leaves from top to bottom	Length along axis (mm)	Thickness of leaves (mm)	Repetition factor
Leaf 1	17.13	0.250	2
Leaf 2	24.56	0.286	2
Leaf 3	32.67	0.330	2
Leaf 4	48.71	0.430	2
Leaf 5	48.80	0.430	2
Leaf 6	51.93	0.450	2
Leaf 7	52.10	0.450	2
Leaf 8	58.89	0.490	2
Leaf 9	63.00	0.545	2

Flower Sample Specifications		
Maximum diagonal length (mm)	Thickness of flower (mm)	Repetition factor
36.23	0.5	1

Stem Sample Specifications			
Vertical length of the cone (mm)	Base radius (mm)	Top radius (mm)	Repetition factor
140.3	2.00	0.50	1

footprints of leaf and flower samples have been imported and further extruded for making three-dimensional models in CST Microwave Studio 2014 (CST MWS 2014) [49]. Subsequently, initial three-dimensional leaf model has been replicated, scaled, and rotated eighteen times around a conical stem at different heights along with a three-dimensional flower structure on top of the plant prototype. Detailed specifications of typical *Catharanthus roseus* plant model (2.70 g mass) are incorporated in Table 3, and designed three-dimensional CAD model is illustrated in Fig. 2.

3.2. Computational Electromagnetic Scheme for SAR Evaluation

SAR simulations for *Catharanthus roseus* plant model have been performed using transient solver available in CST MWS 2014 [49]. Complicated nature of the plant structure shown in Fig. 2 along with lossy low quality factor of the layer permittivities has led to the choice of Time Domain (TD) solver for a robust meshing. The TD solver works based on a computational scheme known as Finite Integration Technique (FIT) developed in 1977 [50, 51]. In this technique, Maxwell's integral equations in the solution space are discretized and solved numerically. Spatial discretizations have been performed with hexahedral meshes of variable sizes, and one wavelength of spatial distance is subdivided into 20 parts. Four perfectly matched layers (PML) with 0.0001 reflection coefficient have been set as electromagnetic boundary at 3 cm distance from the plant structure to bring the plane wave excitation as close as possible. To observe frequency domain characteristics, an inverse transformation accuracy of -40 dB has been chosen which transforms the domain once the steady state energy criterion is met. IEEE/IEC 62704-1 averaging method has been adopted for SAR data calculation with an average mesh cell of 0.00043 g [52]. Once electric field values on all edges of a particular grid cell are known, electric field values on all edges parallel to a particular axis are averaged; this technique is applied to obtain average electric fields along all three axes, and effective electric field strength is calculated at the centre of that

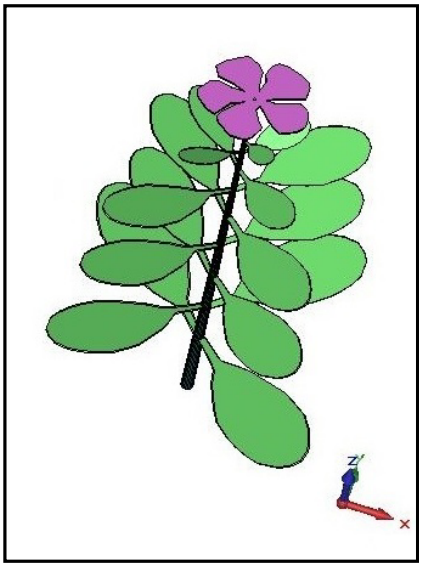

Figure 2. Simplified three dimensional model of *Catharanthus roseus* plant designed in CST MWS 2014 [49].

grid cell. At last, point SAR is calculated using the standard formula $\sigma|E|^2/2\rho$. For SAR averaging, a cubical volume centred at a particular grid cell is expanded evenly in all directions until the target averaging mass is achieved. In special cases, the averaging cube may include partial background material near boundary (maximum 10 percent volume of the cube); however, the mass of background material is not considered to achieve the target mass. This is how spatial averaged SAR value is assigned to a particular 'valid' grid cell in accordance with IEEE/IEC 62704-1 protocol. Other grid cells encompassed in that averaging cube are flagged as 'used' — but partially covered grid cells are marked as 'unused'. This technique is repeated keeping every grid cell at the centre, and grid cells are flagged as 'valid', 'used' or 'unused'. The 'used' grid cells that have never been at the centre of a 'valid' averaging cube are assigned the highest spatial average SAR value among all averaging cubes in which they were enclosed.

For each 'unused' grid cell, six cubical volumes are constructed to achieve the averaging mass by keeping each surface of an 'unused' cell at the centre of a surface of those six averaging cubes. Then, those six cubes are expanded until the target mass is achieved regardless the amount of enclosed background material. Spatial average SAR values of cubes whose volume is not greater than 5 percent of the smallest cube are considered — finally, the highest spatial average SAR value among those averaging cubes is assigned to the 'unused' cell. Then, spatial averaged SAR distribution on the plant surface is derived from spatial average SAR values of individual grid cells that are lying on surface of the designed plant model. The same technique can also be followed to obtain the spatial averaged SAR distribution on any cut plane inside the plant model. Thus, 1 g averaged SAR distribution is obtained on two-dimensional surface of the plant model [52].

4. DISCREPANCIES AMONG DIFFERENT GLOBAL AND NATIONAL ELECTROMAGNETIC REGULATORY STANDARDS

Based on the technical background, motivations, duration of exposure, medical practices and sense of precaution, global and national electromagnetic regulatory standards substantially differ across geographical boundaries [11]. Prescribed plane wave equivalent reference power density levels for public exposure differ by ten to hundred folds depending upon electromagnetic regulatory standards in effect [1, 2, 4, 5]; the discrepancies in prescribed plane wave equivalent reference power density levels are illustrated in Table 4. Public exposure standards in countries like Russia, Italy, etc. (fixed at $0.10\,\mathrm{W/m^2}$ from $\leq 300\,\mathrm{MHz}$ to $300\,\mathrm{GHz}$) are stringent and close enough to the Swiss public standard — therefore, those national electromagnetic standards are not discussed separately [5–8]. However, it should still be

Table 4. Comparative overview of different global and national electromagnetic regulatory standards [1, 2, 4, 5].

Frequency (MHz)	Plane wave equivalent reference power density (W/m^2)					
	Occupational		Public			
	FCC	ICNIRP	FCC	ICNIRP	India	Swiss
947.5	31.58	23.69	6.32	4.74	0.47	0.047
1842.5	50	46.06	10	9.21	0.92	0.092
2150	50	50	10	10	1	0.1
2350	50	50	10	10	1	0.1
2450	50	50	10	10	1	0.1

remembered that no global or national electromagnetic standards have been prepared based on safety of plants.

5. COMPUTED SAR DATA AND ANALYSIS

SAR data along with their distributions in *Catharanthus roseus* plant model have been simulated for occupational and public exposure scenarios in accordance with global electromagnetic standards prescribed by FCC and ICNIRP [1, 2]; moreover, SAR data have also been evaluated as per stricter public exposure standards effective in India and Switzerland [4, 5].

Linearly polarized plane wave (with frequency specified field strength) impinges on the plant model in each SAR simulation scenario. Maximum values of local point SAR (MLP SAR), 1 g averaged SAR, 2 g averaged SAR, and Whole Body Averaged SAR (WBA SAR) have been simulated for above mentioned plant model at 947.5 MHz, 1842.5 MHz, 2150 MHz, 2350 MHz, and 2450 MHz, respectively.

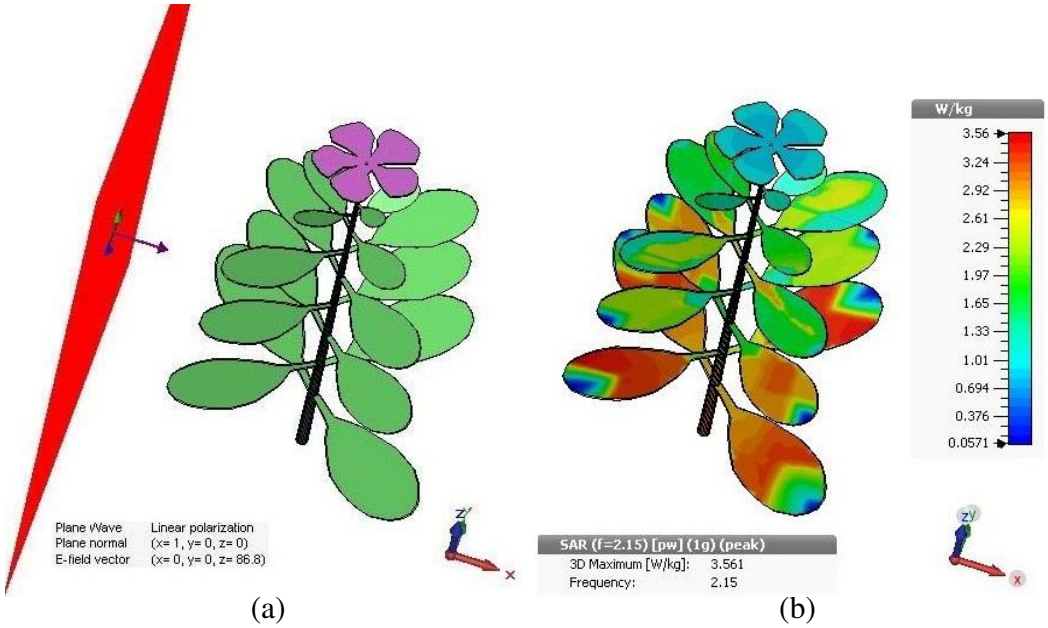

Figure 3. (a) A linearly polarized plane wave passes through *Catharanthus roseus* plant model at 2150 MHz with field strength set as per FCC guidelines for public zone. (b) Evaluated 1 g averaged SAR profile on surface of *Catharanthus roseus* model at 2150 MHz.

Figure 3(a) illustrates a typical simulation setup where a linearly polarized plane wave impinges on designed *Catharanthus roseus* plant model at 2150 MHz as per FCC public exposure guidelines. Fig. 3(b) illustrates consequent 1 g averaged SAR distribution profile on surface of the plant model. Elevated SAR distribution levels are noted among larger leaves at 2150 MHz. It is so because primarily leaves are very thin with sharp edges; moreover, *Catharanthus roseus* leaves possess permittivity of 53.53 at 2150 MHz whereas realized wavelength inside leaf tissue is around $13.95/(53.53)^{1/2}$ cm = 1.9 cm. As a consequence, leaves having dimensions larger than realized wavelength possess higher number of peaks and higher SAR distribution than the rest of the plant structure.

Charge accumulation on surface area with greater curvature tends to be greater in magnitude; this phenomenon can be proved by solving Poisson's equation on and around the surface of an arbitrarily shaped structure [53]. Local electric field strength because of such a nonuniform charge distribution also follows a similar distribution i.e., electric field at points with greater charge density is greater in magnitude [54]. The occurrence of concentrated electric field near sharp edges not only is limited to conducting bodies but also applies to lossy dielectric bodies with finite conductivity [55]. Explanation of scattering problem illustrated by scattering of incident electromagnetic field by a lossy dielectric object ultimately leads to an electric field distribution or equivalent induced surface current density

Table 5. Comparative SAR data for *Catharanthus roseus* plant model at 947.5 MHz as per different global and national electromagnetic regulatory guidelines.

Frequency 947.5 MHz						
Exposure Zone	Occupational		Public			
Guidelines	FCC	ICNIRP	FCC	ICNIRP	India	Swiss
Power density (W/m^2)	31.58	23.69	6.32	4.74	0.47	0.047
Equivalent peak electric field (V/m)	154.3	133.6	69.02	59.77	18.82	5.95
MLP SAR	17.8	13.3	3.56	2.67	0.27	0.027
1 g SAR	5.41	4.06	1.08	0.81	0.08	0.008
2 g SAR	3.81	2.86	0.76	0.57	0.06	0.006
WBA SAR	3.32	2.49	0.66	0.50	0.05	0.005

Table 6. Comparative SAR data for *Catharanthus roseus* plant model at 1842.5 MHz as per different global and national electromagnetic regulatory guidelines.

Frequency 1842.5 MHz						
Exposure Zone	Occupational		Public			
Guidelines	FCC	ICNIRP	FCC	ICNIRP	India	Swiss
Power density (W/m^2)	50	46.06	10	9.21	0.92	0.092
Equivalent peak electric field (V/m)	194.14	186.33	86.82	83.33	26.35	8.33
MLP SAR	46.28	42.63	9.26	8.53	0.85	0.085
1 g SAR	14.34	13.21	2.87	2.64	0.26	0.026
2 g SAR	9.83	9.06	1.97	1.81	0.18	0.018
WBA SAR	8.33	7.68	1.67	1.54	0.15	0.015

Table 7. Comparative SAR data for *Catharanthus roseus* plant model at 2150 MHz as per different global and national electromagnetic regulatory guidelines.

Frequency 2150 MHz						
Exposure Zone	Occupational		Public			
Guidelines	FCC	ICNIRP	FCC	ICNIRP	India	Swiss
Power density (W/m^2)	50	50	10	10	1	0.1
Equivalent peak electric field (V/m)	194.14	194.14	86.82	86.82	27.45	8.68
MLP SAR	57.23	57.23	11.44	11.44	1.14	0.114
1 g SAR	17.80	17.80	3.56	3.56	0.356	0.036
2 g SAR	12.04	12.04	2.41	2.41	0.241	0.024
WBA SAR	10.08	10.08	2.02	2.02	0.202	0.020

Table 8. Comparative SAR data for *Catharanthus roseus* plant model at 2350 MHz as per different global and national electromagnetic regulatory guidelines.

Frequency 2350 MHz						
Exposure Zone	Occupational		Public			
Guidelines	FCC	ICNIRP	FCC	ICNIRP	India	Swiss
Power density (W/m^2)	50	50	10	10	1	0.1
Equivalent peak electric field (V/m)	194.14	194.14	86.82	86.82	27.45	8.68
MLP SAR	66.75	66.75	13.35	13.35	1.34	0.133
1 g SAR	20.85	20.85	4.17	4.17	0.417	0.042
2 g SAR	13.94	13.94	2.79	2.79	0.279	0.028
WBA SAR	11.59	11.59	2.32	2.32	0.232	0.023

that prefers the sharp edges, i.e., magnitude of the distribution is greater in close vicinity of greater surface curvature.

Data summarized in Table 5 to Table 9 indicate that MLP SAR, 1 g averaged SAR and WBA SAR values increase with frequency for all electromagnetic standards. Estimated SAR data increase with frequency primarily because of two factors; first, plane wave equivalent reference power density level increases with increase in frequency of exposure. In addition, effective wavelength within plant dielectric tissue shortens with increase in frequency of exposure; consequently, a higher number of peaks of electric field is developed within the plant model resulting in increased SAR value for even same magnitude of electromagnetic field [33–40]. Moreover, dielectric properties of plant tissues also vary with frequency which further contributes to altering SAR data. Plants are exposed to mobile tower radiation throughout their lifespan — therefore, simulated SAR data are absolutely pertinent and should not be underestimated further by averaging over six minutes of time span.

Comprehensive analyses of data at any particular frequency reveal that there are wide discrepancies among SAR values depending upon the electromagnetic standards in effect. Six different electromagnetic exposure scenarios have been considered during this comparative study — two are global occupational exposure scenarios, and the rest are global as well as national public exposure scenarios [1, 2, 4, 5]. FCC

Table 9. Comparative SAR data for *Catharanthus roseus* plant model at 2450 MHz as per different global and national electromagnetic regulatory guidelines.

Frequency 2450 MHz						
Exposure Zone	Occupational		Public			
Guidelines	FCC	ICNIRP	FCC	ICNIRP	India	Swiss
Power density (W/m^2)	50	50	10	10	1	0.1
Equivalent peak electric field (V/m)	194.14	194.14	86.82	86.82	27.45	8.68
MLP SAR	72.76	72.76	14.55	14.55	1.46	0.145
1 g SAR	22.63	22.63	4.52	4.52	0.45	0.045
2 g SAR	15.05	15.05	3.01	3.01	0.30	0.030
WBA SAR	12.48	12.48	2.50	2.50	0.25	0.025

and ICNIRP prescribing occupational exposure levels are fivefold liberal compared to respective public exposure levels [1, 2]. As a consequence, SAR data for the plant model are extremely high in occupational exposure scenarios at all frequencies. Occupational electromagnetic standards prescribed by FCC and ICNIRP are somewhat different at 900 MHz and 1800 MHz bands; proportionate differences between respective SAR data are also noted (Table 5 and Table 6). SAR data rise by 33 percent (947.5 MHz) and 8 percent (1842.5 MHz) as per FCC occupational standards compared to ICNIRP occupational standards.

In public exposure scenario, plane wave equivalent reference power density levels differ by tenfold to hundredfold among different global and national electromagnetic standards. Resembling occupational exposure scenario, FCC and ICNIRP prescribed public electromagnetic standards are also dissimilar at 900 MHz and 1800 MHz bands, but national public exposure standards in India and Switzerland are much stricter than global scenarios [1, 2, 4, 5]. While analyzing, significant disparity in SAR data is observed among different global and national public exposure standards. Similar to occupational exposure scenario at 947.5 MHz and 1842.5 MHz, SAR data differ by the same ratio between two global public standards (Table 5 and Table 6). However compared to global public standards, all SAR values are reduced by tenfold and hundredfold respectively in India and Switzerland. Fig. 4 illustrates severe contrast in 1 g averaged SAR data as per different global and national public electromagnetic standards.

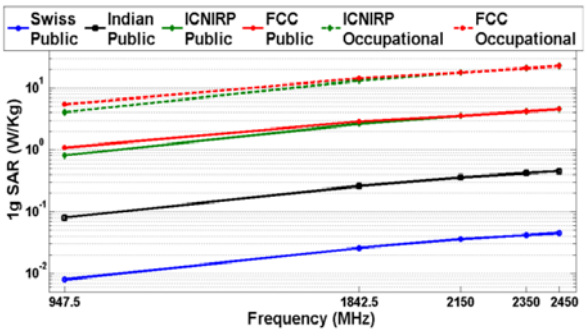

Figure 4. Contrast in 1 g averaged SAR data for *Catharanthus roseus* plant model due to variation among different global and national electromagnetic standards.

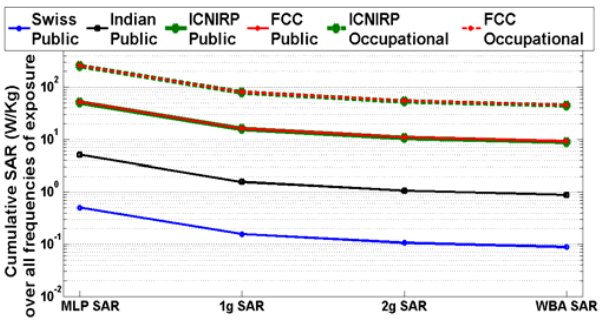

Figure 5. Contrast in cumulative SAR data for *Catharanthus roseus* plant model due to variation among electromagnetic standards prescribed by different global and national organizations.

1 g averaged SAR values at public places are extremely high as per FCC and ICNIRP standards, moderate in India and extremely less in Switzerland. Furthermore, it can be noted that SAR values at public places in countries like Russia, Italy, etc. would also be very much similar to that of Swiss public scenario — as plane wave equivalent reference power density levels are close enough at 947.5 MHz and 1842.5 MHz and exactly the same thereafter [5–8].

Coexistence of several frequency bands results in cumulative SAR effect — base station antennas radiating at different frequencies are operational simultaneously over the years. As a consequence, evaluated SAR data at all frequencies add up and result in cumulative effect in any biological object, and this plant model is no exception. Cumulative SAR data over all five frequencies are illustrated in Fig. 5, and resulting curves indicate substantial discrepancies among different global and national electromagnetic guidelines.

6. CONCLUSIONS

Significant contrast in SAR data is noted for *Catharanthus roseus* plant model due to lack of uniformity among different global and national electromagnetic standards [1, 2, 4, 5]. SAR data for the plant model decrease by tenfold to hundredfold as per Indian and Swiss public standards respectively compared to other established global standards. It is so because both power density ($|E_{inc}|^2/2\eta$) and SAR ($\sigma|E|^2/2\rho$) vary proportionately with the second power of electric field strength; $|E_{inc}|$ and η respectively stand for the maximum amplitude of incident electric field and intrinsic impedance of free space (377 ohm). All SAR data for designed *Catharanthus roseus* model (stands along z-axis) are reported due to linearly polarized plane wave incidence with the direction of propagation along x-axis and electric field variation along z-axis. However, SAR data are expected to change for different directions of propagation or different axes of electric field variation [56]. Reported simulation data can be a good reference for validation through practical SAR measurement. *Catharanthus roseus* tissue equivalent phantom liquids are prepared for the same purpose.

The observed wide variation in SAR data due to lack of uniformity among different electromagnetic standards is not object specific, i.e., this contrast in SAR data is applicable to all biological models irrespective of their structures and tissue layer distributions. Hence, introducing uniform electromagnetic standards worldwide is an absolute necessity considering effects of electromagnetic energy absorption in plants (along with humans). Basis to introduce decisive uniform electromagnetic standards is a trade-off between two factors. Minimum feasible power density (or equivalent electric field strength) sufficient for seamless data and voice connectivity over-the-air is the primary factor. This factor further depends on the effective implementation of smaller cell size and more frequency reuses; more mobile towers should be installed, and each mobile tower antenna must emit minimal electromagnetic power to reduce radiated power density in far field. Secondly, further investigations should be carried out to explore the maximum power density levels over different frequency bands that have negligible biological effects on humans as well as plants. Different global and national electromagnetic standards are consistent with their own history, evolution criteria, and the policy promoted by the issuing authority. All those regulatory bodies must decide together a standard set of criteria for investigating biological effects of electromagnetic radiation on humans and plants. Scientific publications that report investigations in accordance with those standard sets of criteria will have to be taken into consideration – thus, the regulatory specifications can be harmonized and lead to subsequent introduction of a globally uniform electromagnetic standards [11]. However until biological effects are precisely known, the minimum feasible power density sufficient for seamless data and voice connectivity should be treated as the reference level and lead the path toward uniform electromagnetic regulatory standards worldwide.

ACKNOWLEDGMENT

Authors would like to acknowledge School of Nuclear Studies and Application, Jadavpur University for providing open ended coaxial dielectric measurement kit to Electronics and Telecommunication Engineering department, Jadavpur University. Authors are also thankful to Mr. Amartya Banerjee and Dr. Kaushik Patra for their suggestions in framing and presenting the research work.

Last but not the least, authors would also like to acknowledge Rashtriya Uchchatar Shiksha Abhiyan 2.0 scheme (Govt. of India) at Jadavpur University (Internal Project Ref. No. R-11/269/19) for funding the research work.

REFERENCES

1. Cleveland, Jr., R. F., D. M. Sylvar, and J. L. Ulcek, "Evaluating compliance with FCC guidelines for human exposure to radiofrequency electromagnetic fields," *FCC OET Bulletin*, Vol. 65, Edition 97-01, Washington D.C., 1997.
2. ICNIRP, "Guidelines for limiting exposure to electromagnetic fields (100 kHz to 300 GHz)," *Health Phys.*, Vol. 118, No. 5, 483–524, 2020.
3. IEEE, "IEEE standard for safety levels with respect to human exposure to electric, magnetic, and electromagnetic fields, 0 Hz to 300 GHz," *IEEE Std C95.1-2019 (Revision of IEEE Std C95.1-2005/Incorporates IEEE Std C95.1-2019/Cor 1-2019)*, 1–312, United States, 2019.
4. DoT, *Mobile Communication — Radio Waves & Safety*, 1–15, India, 2012.
5. SAEFL, *Electrosmog in the Environment*, 1–56, Switzerland, 2005.
6. Ministry of Health of the Russian Federation, "SanPiN 2.1.8/2.2.4.1190-03: Arrangement and operation of land mobile radiocommunication facilities — Hygienic requirements," 1–17, Russia, 2003.
7. The president of the council of ministers (Italy), "Establishment of exposure limits, attention values, and quality goals to protect the population against electric, magnetic, and electromagnetic fields generated at frequencies between 100 kHz and 300 GHz," 1–6, unofficial translation by P. Vecchia, Italy, 2003.
8. Vecchia, P., "Radiofrequency fields: Bases for exposure limits," *2 European IRPA Congress on Radiation Protection — Radiation Protection: From Knowledge to Action*, 1–19, Paris, 2006.
9. Mazar, H., "A global survey and comparison of different regulatory approaches to non-ionizing RADHAZ and spurious emissions," *IEEE International Conference on Microwaves, Communications, Antennas and Electronics Systems (COMCAS)*, 1–6, Tel Aviv, 2009.
10. Kumar, G., *Report on Cell Tower Radiation*, submitted to secretary, 1–50, DoT, India, 2010.
11. Foster, K. R., "Exposure limits for radiofrequency energy: Three models," *Proceedings of the Eastern European Regional EMF Meeting and Workshop (Criteria for EMF Standards Harmonization)*, 1–6, Varna, Bulgaria, 2001.
12. Stuchly, S. S., M. A. Stuchly, A. Kraszewski, and G. Hartsgrove, "Energy deposition in a model of man: Frequency effects," *IEEE Trans. Biomedical Engineering*, Vol. 33, No. 7, 702–711, 1986.
13. Gultekin, D. H. and P. H. Siegel, "Absorption of 5G radiation in brain tissue as a function of frequency, power and time," *IEEE Access*, Vol. 8, 115593–115612, 2020.
14. Meier, K., V. Hombach, R. Kästle, R. Y. Tay, and N. Kuster, "The dependence of electromagnetic energy absorption upon human-head modelling at 1800 MHz," *IEEE Trans. Microwave Theory and Techniques*, Vol. 45, No. 11, 2058–2062, 1997.
15. Christ, A., A. Klingenböck, T. Samaras, C. Goiceanu, and N. Kuster, "The dependence of electromagnetic far-field absorption on body tissue composition in the frequency range from 300 MHz to 6 GHz," *IEEE Trans. Microwave Theory and Techniques*, Vol. 54, No. 5, 2188–2195, 2006.
16. Cooper, J., B. Marx, J. Buhl, and V. Hombach, "Determination of safety distance limits for a human near a cellular base station antenna, adopting the IEEE standard or ICNIRP guidelines," *Bioelectromagnetics*, Vol. 23, No. 6, 429–443, 2002.
17. Takei, R., T. Nagaoka, K. Saito, S. Watanabe, and M. Takahashi, "SAR variation due to exposure from a smartphone held at various positions near the torso," *IEEE Trans. Electromagnetic Compatibility*, Vol. 59, No. 2, 747–53, 2017.
18. Gandhi, O. P., "Yes the children are more exposed to radiofrequency energy from mobile telephones than adults," *IEEE Access*, Vol. 3, 985–988, 2015.

19. Karunarathna, M. A. A. and I. J. Dayawansa, "Energy absorption by the human body from RF and microwave emissions in Sri Lanka," *Sri Lankan J. of Phys.*, Vol. 7, 35–47, 2006.
20. Hirata, A., S. Kodera, J. Wang, and O. Fujiwara, "Dominant factors influencing whole-body average SAR due to far-field exposure in whole-body resonance frequency and GHz regions," *Bioelectromagnetics*, Vol. 28, No. 6, 484–487, 2007.
21. Hirata, A., N. Ito, O. Fujiwara, T. Nagaoka, and S. Watanabe, "Conservative estimation of whole-body-averaged SARs in infants with a homogeneous and simple-shaped phantom in the GHz region," *Phys. in Med. and Biol.*, Vol. 53, No. 24, 7215–7223, 2008.
22. Iyama, T., T. Onishi, Y. Tarusawa, S. Uebayashi, and T. Nojima, "Novel specific absorption rate (SAR) measurement method using a flat solid phantom," *IEEE Trans. Electromagnetic Compatibility*, Vol. 50, No. 1, 43–51, 2008.
23. Taguchi, K., L. Laakso, K. Aga, A. Hirata, Y. Diao, J. Chakarothai, and T. Kashiwa, "Relationship of external field strength with local and whole-body averaged specific absorption rates in anatomical human models," *IEEE Access*, Vol. 6, 70186–70196, 2018.
24. Wessapan, T., S. Srisawatdhisukul, and P. Rattanadecho, "Specific absorption rate and temperature distributions in human head subjected to mobile phone radiation at different frequencies," *Int. J. of Heat and Mass Transfer*, Vol. 55, No. 1–3, 347–359, 2012.
25. Wessapan, T. and P. Rattanadecho, "Specific absorption rate and temperature increase in the human eye due to electromagnetic fields exposure at different frequencies," *Int. J. of Heat and Mass Transfer*, Vol. 64, 426–435, 2013.
26. Kraszewski, A. W., S. Trabelsi, and S. O. Nelson, "Broadband microwave wheat permittivity measurement in free space," *J. of Microwave Power and Electromagnetic Energy*, Vol. 37, No. 1, 41–54, 2002.
27. Wee, F. H., P. J. Soh, A. H. M. Suhaizal, H. Nornikman, and A. A. M. Ezanuddin, "Free space measurement technique on dielectric properties of agricultural residues at microwave frequencies," *2009 SBMO/IEEE MTT-S International Microwave and Optoelectronics Conference (IMOC)*, 183–187, Belem, 2009.
28. Nelson, S. O., "Measuring dielectric properties of fresh fruits and vegetables," *IEEE Antennas and Propagation Society International Symposium 2003*, 46–49, Columbus, 2003.
29. Guo, W., S. O. Nelson, S. Trabelsi, and S. J. Kays, "10–1800 MHz dielectric properties of fresh apples during storage," *J. of Food Engg.*, Vol. 83, No. 4, 562–569, 2007.
30. Nelson, S. O. and S. Trabelsi, "Dielectric spectroscopy measurements on fruit, meat, and grain," *Trans. of the ASABE*, Vol. 51, No. 5, 1829–1834, 2008.
31. Kundu, A. and B. Gupta, "Broadband dielectric properties measurement of some vegetables and fruits using open ended coaxial probe technique," *Proceedings of The 2014 International Conference on Control, Instrumentation, Energy and Communication (CIEC)*, 480–484, Kolkata, 2014.
32. Mavrovic, A., A. Roy, A. Royer, B. Filali, F. Boone, C. Pappas, and O. Sonnentag, "Dielectric characterization of vegetation at L band using an open-ended coaxial probe," *Geoscientific Instrumentation, Methods and Data Systems*, Vol. 7, No. 3, 195–208, 2018.
33. Kundu, A., "Specific absorption rate evaluation in apple exposed to RF radiation from GSM mobile towers," *IEEE Applied Electromagnetics Conference (AEMC) 2013*, 1–2, Bhubaneswar, 2013.
34. Kundu, A., *RF Energy Absorption in Plant Parts due to Cell Tower Radiation*, Lambert Academic Publishing, Germany, 2015.
35. Kundu, A. and B. Gupta, "SAR evaluation of apple as per FCC RF exposure guideline," *Recent Development in Electrical, Electronics and Engineering Physics (RDE3P-2013)*, 152–156, MCKVIE, India, 2013.
36. Kundu, A. and B. Gupta, "Comparative SAR analysis of some Indian fruits as per the revised RF exposure guideline," *IETE J. of Res.*, Vol. 60, No. 4, 296–302, 2014.
37. Kundu, A., B. Gupta, and A. I. Mallick, "SAR analysis in a typical bunch of grapes exposed to radio frequency radiation in Indian scenario," *IEEE International Conference on Microelectronics, Computing and Communication (MicroCom2016)*, 1–5, India, 2016.

38. Kundu, A., B. Gupta, and A. I. Mallick, "Specific absorption rate calculation in a typical bunch of Sapodilla fruits (*Manilkara zapota*) as per revised Indian RF exposure guidelines," *3rd URSI Regional Conference on Radio Science (URSI-RCRS)*, URSI, India, 2017.
39. Kundu, A. and B. Gupta, "Review on cell tower radiation absorption in Indian flora and related consequences: A critical issue for sustainable telecom growth," *National Conference on Sustainable Technology to Connect People with Nature*, Kolkata, 2017.
40. Kundu, A., B. Gupta, and A. I. Mallick, "Specific absorption rate evaluation in a typical multilayer fruit: Coconut with twig due to electromagnetic radiation as per Indian standards," *Microwave Review*, Vol. 23, No. 2, 24–32, 2017.
41. Deschamps, G., "Impedance of an antenna in a conducting medium," *IRE Trans. Antennas and Propagation*, Vol. 10, No. 5, 648–650, 1962.
42. Liu, L., D. Xu, and Z. Jiang, "Improvement in dielectric measurement technique of open-ended coaxial line resonator method," *Electronics Letters*, Vol. 22, No. 7, 373–375, 1986.
43. Xu, D., L. Liu, and Z. Jiang, "Measurement of the dielectric properties of biological substances using an improved open-ended coaxial line resonator method," *IEEE Trans. Microwave Theory and Techniques*, Vol. 35, No. 12, 1424–1428, 1987.
44. Stuchly, M. A. and S. S. Stuchly, "Coaxial line reflection method for measuring dielectric properties of biological substances at radio and microwave frequencies — A review," *IEEE Trans. Instrum. Meas.*, Vol. 29, No. 3, 176–183, 1980.
45. Athey, T. W., M. A. Stuchly, and S. S. Stuchly, "Measurement of radio frequency permittivity of biological tissues with an open-ended coaxial line: Part I," *IEEE Trans. Microwave Theory and Techniques*, Vol. 30, No. 1, 82–86, 1982.
46. Zajíček, R., J. Vrba, and K. Novotný, "Evaluation of a reflection method on an open-ended coaxial line and its use in dielectric measurements," *Acta Polytechnica*, Vol. 46, No. 5, 50–54, 2006.
47. Zajíček, R., L. Oppl, and J. Vrba, "Broadband measurement of complex permittivity using reflection method and coaxial probes," *Radioengineering*, Vol. 17, No. 1, 14–19, 2008.
48. Bobowski, J. S. and T. Johnson, "Permittivity measurements of biological samples by an open-ended coaxial line," *Progress In Electromagnetics Research B*, Vol. 40, 159–183, 2012.
49. CST STUDIO SUITE 2014, https://www.3ds.com/products-services/simulia/products/cst-studio-suite/, (Accessed Sept. 6, 2019).
50. Weiland, T., "A discretization method for the solution of Maxwell's equations for six-component fields," *Electronics and Communications AEU*, Vol. 31, No. 3, 116–120, 1977.
51. Clemens, M. and T. Weiland, "Discrete electromagnetism with the finite integration technique," *Progress In Electromagnetics Research*, Vol. 32, 65–87, 2001.
52. "IEC/IEEE International Standard — Determining the peak spatial-average specific absorption rate (SAR) in the human body from wireless communications devices, 30 MHz to 6 GHz — Part 1: General requirements for using the finite-difference time-domain (FDTD) method for SAR calculations," *IEC/IEEE 62704-1: 2017*, 1–86, United States, 2017.
53. Bhattacharya, K., "On the dependence of charge density on surface curvature of an isolated conductor," *Physica Scripta*, Vol. 91, No. 3, 035501, 2016.
54. Jordan, E. C. and K. G. Balmain, *Electromagnetic Waves and Radiating Systems*, 2nd Edition, PHI Learning, New Delhi, 2009.
55. Deshpande, M. D., C. R. Cockrell, F. B. Beck, E. Vedeler, and M. B. Koch, "Analysis of electromagnetic scattering from irregularly shaped, thin, metallic flat plates," *NTRS — NASA Technical Reports Server*, NASA Technical Paper 3361, 1993.
56. Kundu, A., B. Gupta, and A. I. Mallick, "Dependence of electromagnetic energy distribution inside a typical multilayer fruit model on direction of arrival and polarization of incident field," *2019 IEEE Radio and Antenna Days of the Indian Ocean (RADIO)*, 1–2, Reunion, 2019.